EMBO reports

scientific report

Structure and oligomeric state of human transcription factor TFIIE

Anass Jawhari[1], Muriel Uhring[1]*, Sacha De Carlo[1†], Corinne Crucifix[1,2], Guiseppe Tocchini-Valentini[1], Dino Moras[1], Patrick Schultz[1,2+] & Arnaud Poterszman[1]*

[1]Department of Structural Biology and Genomics, Institut de Génétique et de Biologie Moléculaire et Cellulaire, CNRS/INSERM/ULP, Illkirch, France, and [2]Ecole Supérieure de Biotechnologie de Strasbourg, Pôle API, Illkirch, France

The general RNA polymerase II transcription factor TFIIE, which is composed of two subunits, has essential roles in both transcription initiation and promoter escape. Electron microscopy analysis of negatively stained human TFIIE showed a large proportion of α/β heterodimers as well as a small proportion of tetramers. Analytical ultracentrifugation, chemical crosslinking, pulldown experiments and cryo-electron microscopy confirmed that TFIIE is a α/β heterodimer in solution. Three-dimensional envelopes of the α/β particles showed an elongated structure composed of three distinct modules. Finally, a model for the quaternary architecture of the complex is proposed that provides a structural framework to discuss the function of TFIIE in the context of RNA polymerase II transcription initiation.

Keywords: transcription; TFIIE; electron microscopy; oligomeric state; solution studies

EMBO reports (2006) 7, 500–505. doi:10.1038/sj.embor.7400663

INTRODUCTION

In eukaryotes, transcription of protein-coding genes requires RNA polymerase II (RNA Pol II) and five general transcription factors, TFIIB, TFIID, TFIIF, TFIIE and TFIIH, to form the preinitiation complex (PIC). TFIIE is composed of two highly charged subunits with a molecular mass of 56 kDa (TFIIEα) and 34 kDa (TFIIEβ; Ohkuma *et al*, 1990; Fig 1A). The two subunits interact through interfaces comprising the amino-terminal part of TFIIEα and residues 193–238 of TFIIEβ (Ohkuma *et al*, 1995; Okamoto *et al*, 1998). Order-of-addition experiments demonstrated that TFIIE enters the PIC after RNA Pol II and interacts directly with the unphosphorylated form of RNA Pol II, with TFIIB and with both subunits of TFIIF (Orphanides *et al*, 1996; Roeder, 1996). TFIIE is required for the recruitment of TFIIH and for the regulation of its kinase and helicase activities (Lu *et al*, 1992; Ohkuma & Roeder, 1994). The TFIIE α-subunit is required for the specific interaction with TFIIH. The regions of interactions were mapped in the acidic carboxyl terminus of TFIIEα and in the conserved zinc-finger domain. The central core region of the β-subunit that binds to double-stranded DNA is essential for basal and activated transcription, and a C-terminal half contains two basic stretches that interact with TFIIB, TFIIFβ and single-stranded DNA (Okamoto *et al*, 1998). Protein–DNA crosslinking experiments showed that both TFIIE subunits bind to the start site of the promoter between positions −10 and +10 (Kim *et al*, 2000), whereas in the absence of sarkosyl (Robert *et al*, 1996) the binding site included also upstream and downstream regions of the start site (−40 to −30 and +10 to +30, respectively).

Three conserved TFIIE modules were solved by X-ray crystallography or NMR. Residues 1–97 of TFE, the archeael homologue of TFIIEα, adopt a winged helix–turn–helix fold (Meinhart *et al*, 2003). The zinc-finger domain of TFIIEα is composed of one α-helix and five β-strands (Okuda *et al*, 2004). Residues 66–146 of the central core domain of TFIIEβ form a domain that resembles winged helix proteins (Okuda *et al*, 2000). Although structural and biochemical information is available for these conserved modules, the complete TFIIE structure has not yet been solved. As a matter of fact, also its oligomeric state is under debate, as gel filtration experiments are consistent with an α2/β2 heterotetramer (Ohkuma *et al*, 1990; Hayashi *et al*, 2005), whereas other experiments argue in favour of a heterodimeric α/β assembly (Sayre *et al*, 1992; Bushnell *et al*, 1996; Itoh *et al*, 2005).

Here we describe the molecular organization of Human TFIIE. A small proportion of tetramers could be observed in negatively stained preparations, but most of the particles corresponded to α/β heterodimers. We confirmed the existence of α/β heterodimers by analytical ultracentrifugation, chemical crosslinking and pulldown experiments. The structure of this dimer was further characterized by cryo-electron microscopy. A three-dimensional (3D) envelope of the α/β particles was determined and showed

[1]Department of Structural Biology and Genomics, Institut de Génétique et de Biologie Moléculaire et Cellulaire, CNRS/INSERM/ULP, rue Laurent Fries, 67404 Illkirch, France
[2]Ecole Supérieure de Biotechnologie de Strasbourg, Pôle API, rue Sébastien Brand, 67404 Illkirch, France
*These authors contributed equally to this work
[†]Present address: Molecular and Cell Biology Department, Howard Hughes Medical Institute, University of California, Berkeley, California, USA
[+]Corresponding author. Tel: +33 3 90 24 4800; Fax: +33 3 88 65 3201;
E-mail: patrick.schultz@igbmc.u-strasbg.fr

Received 4 October 2005; revised 2 November 2005; accepted 20 February 2006; published online 17 March 2006

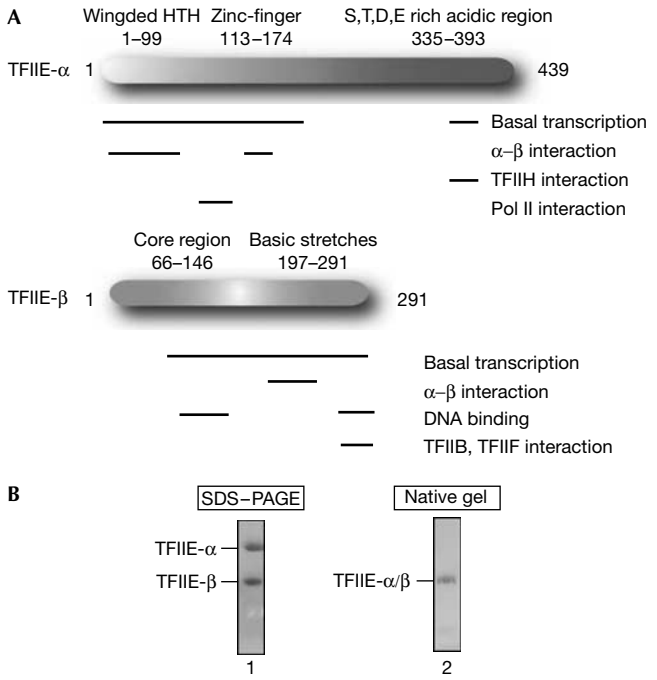

Fig 1 | Human TFIIE subunits. (**A**) Domain organization of human TFIIE. (**B**) Coomassie blue-stained 12.5% SDS and 8–25% native polyacrylamide gel of purified TFIIE.

an elongated structure composed of three distinct modules. We propose a model for the quaternary architecture of TFIIE based on the analysis of a glutathione *S*-transferase (GST)-tagged complex and supported by an immuno-labelling experiment. This model provides a structural framework to the function of TFIIE in the context of RNA Pol II transcription initiation.

RESULTS AND DISCUSSION

To study the molecular architecture of human TFIIE, the α- and β-subunits were coexpressed in *Escherichia coli* and purified. When analysed by SDS–polyacrylamide gel electrophoresis, two bands of equal intensities that correspond to the α- and β-subunits were observed, whereas a single band was detected in native conditions (Fig 1B). Recombinant TFIIE migrated as a single peak in analytical size-exclusion chromatography, with a retention time corresponding to an apparent molecular mass of about 200 kDa, as previously reported (Ohkuma *et al*, 1990; supplementary Fig 1 online).

3D model of human TFIIE

Electron microscopy inspection of negatively stained TFIIE showed different oligomeric states (supplementary Fig 2 online). About 15% of the particles were roughly 12 × 11 nm in size, whereas most of the particles (75%) were medium in size (11 × 6 nm) and elongated. About 10% of the particles were significantly smaller and were not further analysed.

The analysis of 4,480 images of large particles resulted in class averages that clearly showed a two-fold symmetry axis consistent with α2/β2 tetramers (Fig 2A, panels 4,5). A 3D model was calculated from 108 different views and its reprojection matched

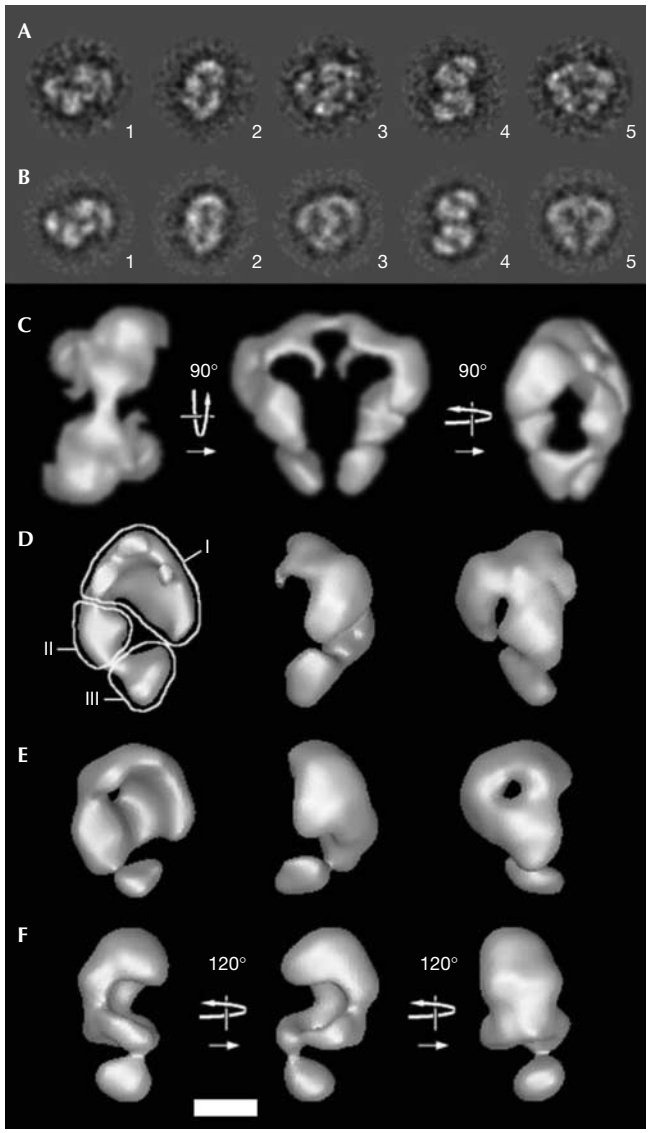

Fig 2 | Three-dimensional models of human TFIIE. (**A**) Negatively stained TFIIE tetramers. (**B**) Corresponding projections of the three-dimensional (3D) tetramer model. (**C**) Surface representation of the TFIIE tetramer. The arrows indicate the relative orientation of the model. (**D**) Model of the α/β TFIIE heterodimer extracted from the tetramer. Modules I, II and III are indicated. (**E**) Envelope of the negatively stained α/β TFIIE heterodimer. (**F**) Envelope of the hydrated α/β heterodimer observed in cryo-negative stain. Scale bar, 11.3 nm (**A**,**B**) and 3.9 nm (**C**–**F**).

the original views (Fig 2B). The symmetrized envelope, the volume of which corresponds to the α2/β2 tetramer, is composed of two α/β heterodimeric molecules (Fig 2C). When viewed down the symmetry axis, each heterodimer has a compact structure about 7.5 × 5 nm in size, whereas they are elongated (11 nm) when viewed from the side. The heterodimer is formed by three distinct modules arranged in an almost closed structure (Fig 2D). The largest module I contains the small (α/β)–(α/β) interaction interface and contacts the central module II, whereas the distal module III is connected to module II by a thin linker.

The analysis of 5,627 medium-sized particles confirmed the absence of any internal symmetry in these complexes and the 3D structure reconstructed from 104 distinct views was similar in shape to the asymmetric unit of the tetramer (Fig 2E). Although small differences are observed between the two models, such as the coalescence of the distal end of module I with module II, these experiments show that the most abundant TFIIE particles are α/β heterodimers.

Oligomeric state of TFIIE in solution

The two oligomeric states observed for negatively stained TFIIE raised the question of the dynamic equilibrium between the two states, as a single state was observed in gel filtration. This heterogeneity could arise from tetramers that fall apart on mounting for electron microscopy or conversely from hetero-dimeric self-assembly during the drying process, as was described for other particles, such as haemocyanin (Wichertjes *et al*, 1989). To examine these possibilities, a suspension of TFIIE was included in a saturated solution of ammonium molybdate, rapidly frozen to preserve the hydration of the molecules and analysed by cryo-electron microscopy (Adrian *et al*, 1998; De Carlo *et al*, 2002). The cryo-negatively stained sample was homogeneous and no large particles showing a *P*2 symmetry could be observed, indicating that in hydrated conditions TFIIE is heterodimeric.

A total of 12,084 molecular images were analysed, and a 3D model including 380 different molecular views was determined independently of the previous analyses. The resolution of the reconstruction was of 1.9 nm (data not shown) and the final model shows the same organization into three modules as found in negative stain (Fig 2F). In the hydrated state, module I is less extended and the separation with module II is less pronounced than in negative stain. Module III is connected to the remaining structure by a thin linker, but its relative orientation is different, suggesting that this module is flexible.

Biochemical and biophysical methods were used to further analyse the oligomeric state of TFIIE in a buffer containing 250 mM NaCl to minimize nonspecific interactions. When TFIIE (Fig 3A, lane 1) was chemically crosslinked with 0.02% glutaraldehyde, a single polypeptide with an estimated molecular mass of 90 kDa corresponding to the α/β heterodimer was generated, whereas no band of higher molecular mass was detected (Fig 3A, lane 2). Pulldown assays were also carried out to test whether tetramers can form in solution. Two differently tagged versions of TFIIEα (FLAG and $(His)_6$) as well as a native TFIIEβ were expressed independently in *E. coli* and then mixed to form chimeric TFIIE complexes. $(His)_6$-tagged TFIIEα should co-precipitate with FLAG–TFIIEα and FLAG–TFIIEβ only if a tetramer is formed and not in case of α/β heterodimers. A similar experiment was performed by monitoring the pulldown of FLAG–TFIIEα with $(His)_6$-tagged TFIIEα on metal affinity beads. In both cases, TFIIEβ was retained on the beads, but no traces of complexes containing both variants of TFIIEα could be detected, thus confirming that tetramers are not stable in these conditions (Fig 3B, compare lanes 3,5,7). Finally, sedimentation equilibrium analysis was carried out. The experimental data fitted best to a single-species model with no traces of multimerization (Fig 3C) and a molecular mass of 84,589±214 Da consistent with the calculated molecular mass of a recombinant αβ heterodimer (84,686 Da).

These experiments establish the presence of an α/β form for human TFIIE in solution and validate the cryo-electron microscopy observations. Similar conclusions were reached by a recent

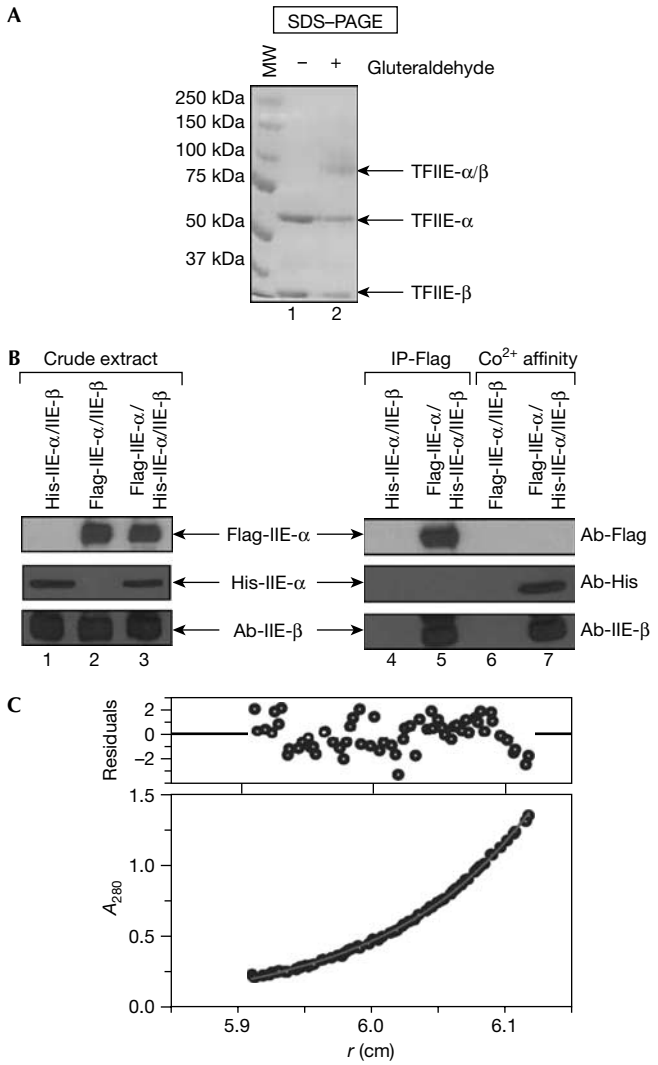

Fig 3 | Oligomeric state of TFIIE. (**A**) Chemical crosslinking. Purified TFIIE (1.0 mg/ml) incubated in the presence of glutaraldehyde (0.02%) for 30 min at 25 °C was analysed by 12.5% SDS–polyacrylamide gel electrophoresis and Coomassie blue stained. (**B**) Co-immunoprecipitation studies of TFIIE. (**C**) Sedimentation equilibrium. Purified TFIIE (1.5 mg/ml) in 20 mM Tris–HCl, 250 mM NaCl and 2 mM β-mercaptoethanol was spun at 12,000 r.p.m. and 20 °C in an XL-A analytical ultracentrifuge with absorbance monitoring. After equilibration, data were fitted using a single component model with nonlinear least square analysis (solid line).

independent study by Itoh *et al* (2005). Our data also reproduce the behaviour of yeast TFIIE that elutes from a gel filtration column with a Stokes radius typical of a 200 kDa globular protein, but sediments in a glycerol gradient as a much smaller protein (Sayre *et al*, 1992). A weak affinity between heterodimers that could result in the formation of tetramers in the conditions experienced in negative stain cannot be excluded.

Molecular organization of TFIIE

As the N-terminal part of TFIIEα was shown to interact with the β-subunit (Ohkuma *et al*, 1995), we were interested to map this

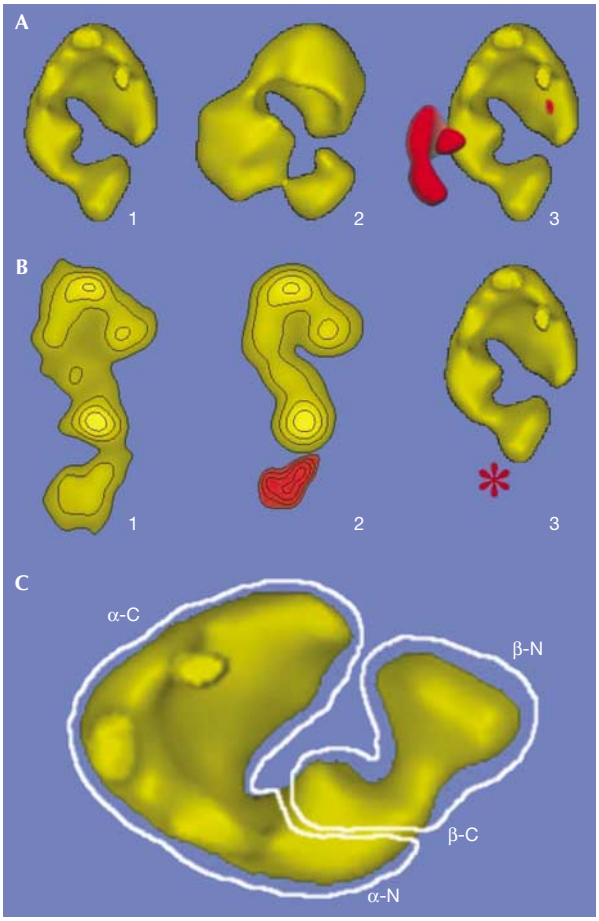

Fig 4 | TFIIE subunit mapping. (**A**) Surface representation of negatively stained native TFIIE (panel 1), TFIIE tagged with glutathione *S*-transferase (GST) at the amino terminus of the α-subunit (panel 2) and of the difference map showing the additional density (red) present in the GST-tagged TFIIE (panel 3). (**B**) Projection of a TFIIE complex FLAG tagged at the N-terminus of the β-subunit and labelled by a FLAG-specific antibody (panel 1), difference map with an unlabelled view of TFIIE (red in panel 2) and location of the N-terminus of TFIIEβ on the three-dimensional model of the particle. (**C**) Quaternary model for the assembly of the α- and β-subunits. The N- and Carboxy-terminal ends of each subunit are indicated.

interface onto the 3D model. A TFIIE complex containing an N-terminally GST-tagged α-subunit and a wild-type β-subunit was purified by GST affinity and size-exclusion chromatography. A total of 8,766 negatively stained particles were recorded and a 3D model was calculated from 187 molecular views (Fig 4A, panel 2). The GST-tagged TFIIE has a three-domain organization similar to the native TFIIE, but with a larger central module II. A density difference map thresholded at 3σ was calculated and showed that module II contains a statistically significant additional density in the GST-tagged TFIIE and that the other differences are not significant (red density in Fig 4A, panel 3). This result shows that the N terminus of TFIIEα and its interaction partner, the C-terminal third of TFIIEβ, are located in module II. TFIIEβ was mapped using a protein FLAG-tagged at the N terminus and probed with anti-FLAG

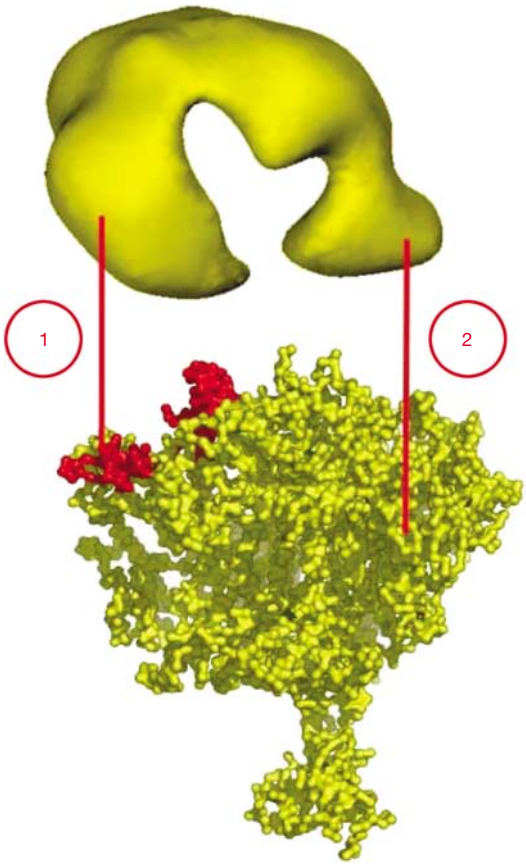

Fig 5 | RNA polymerase–TFIIE interactions. Representation of TFIIE and RNA polymerase II (RNA Pol II) (Protein Data Bank accession code 1NT3) in which Rpb9 is highlighted in red. The documented interactions between TFIIE subunits and RNA Pol II or DNA are shown by connections 1 and 2, respectively.

antibodies. The analysis of 4,691 immune complexes showed that the antibodies bind specifically to module III (Fig 4B).

The quaternary structure of TFIIE is thus represented as a linear arrangement of the α- and β-subunits in which module I contains the C-terminal half of TFIIEα, module II forms the α/β interface, whereas the N terminus of TFIIEβ resides in module III (Fig 4C). Module II is likely to contain the winged HTH module formed by the N terminus of TFIIEα. The almost autonomous module III may correspond to an independent structural fold, most probably the central core domain of TFIIEβ (residues 66–146) that is placed next to the TFIIEα binding interface (Okuda *et al*, 2000).

TFIIE in the PIC

Acting at a late stage in PIC formation, TFIIE interacts with many components of the basal transcription machinery, including TFIIB, TFIIH and Pol II, as well as with the promoter DNA. TFIIEα was reported to interact with the Rpb9 subunit of RNA Pol II, which is located in the jaw region (Van Mullem *et al*, 2002), whereas TFIIEα and TFIIEβ can be photocrosslinked to upstream DNA located 10 nm away from the jaw region. These data can be rationalized by the extended and elongated shape of TFIIE that is suitable to bridge these widely separated positions. In a tentative

orientation of the TFIIE onto RNA Pol II, the α-subunit can interact with Rpb9 (shown in red and connected to TFIIE by line 1 in Fig 5) as well as with the promoter DNA close to the start site and up to the +20 region, whereas the β-subunit is projected upstream of the start site and could interact in the vicinity of the TATA box (Fig 5, connector line 2; Forget *et al*, 2004). The proposed orientation is also consistent with TFIIE–RNA Pol II 2D co-crystals, in which the major density difference was detected in front of the jaws (Leuther *et al*, 1996). Our results indicate that the observed footprints can be explained by the extended shape of TFIIE and do not require the presence of two molecules (Kim *et al*, 2000; Forget *et al*, 2004). However, a more precise description of the path of DNA within the PIC awaits further structural data.

METHODS

Cloning and purification. Complementary DNA encoding human TFIIE subunits (a kind gift from Jean Marc Egly) was inserted into the *Nde*I–*Bam*HI restriction sites of several expression vectors. To produce $(His)_6$–TFIIEα, FLAG–TFIIEα and GST–TFIIEα, the corresponding cDNA was cloned into pET28b, pFLAG-Kan (a p28b derivative in which the $(His)_6$ tag was replaced by a FLAG sequence) and pGEX-NB. To produce TFIIEβ, the corresponding cDNA was cloned into pACYC-11b (Fribourg *et al*, 2001) and pFLAG-Amp (a p15b derivative in which the $(His)_6$ tag was replaced by a FLAG sequence). For production, BL21λ(DE3) cells co-transformed with the $(His)_6$–TFIIEα and $(His)_6$–TFIIEβ or the GST–TFIIEα and GST–TFIIEβ expression plasmids were grown in Luria Broth medium containing the appropriate antibiotics to an A_{600} of 0.8 at 37 °C. The temperature was then shifted to 22 °C for 2 h before addition of 0.4 mM isopropyl-β-D-thiogalactoside and further grown for 12 h. Cells were lysed in buffer A (20 mM Tris–HCl, pH 7.5, 250 mM NaCl, 2 mM β-mercaptoethanol), clarified by centrifugation (45,000 r.p.m. at 4 °C) and the supernatant containing the affinity-tagged α-subunit was then applied onto a metal (Talon, Clontech, Mountain View, CA, USA) or a GST (Amersham, Buckinghamshire, UK) affinity column using 1 ml of beads per litre of cells. After washing with buffer A containing 0.1% NP-40, proteins were eluted with buffer A containing 250 mM imidazol or 20 mM glutathione. TFIIE fractions were concentrated in Centriprep30 (Millipore, Billerica, MA, USA) and loaded on a Superdex S200-16/60 gel filtration (Pharmacia, Buckinghamshire, UK). Typical yields of 1 mg of pure complex per litre of culture were obtained.

Protein pulldown interaction assay. Clarified extracts from cells expressing separately Flag–TFIIEα, His–TFIIEα or TFIIEβ were prepared as described above, mixed at 4 °C for 3 h and incubated either with anti-FLAG (M2, Sigma-Aldrich, St Louis, MO, USA) or with metal affinity beads. After washing with buffer A containing 0.1% NP-40, bound proteins eluted in the same buffer containing either 0.2 mg/ml of FLAG peptide or 250 mM imidazole and were analysed by western blotting using monoclonal antibodies directed against the FLAG tag, the $(His)_6$ tag or TFIIEβ.

Electron microscopy and image processing. TFIIE was negatively stained by a 2% uranyl acetate solution and was imaged on a Philips CM120 transmission electron microscope (TEM) operating at 120 kV with a LaB6 filament at 45,000 magnification. For cryo-negative staining, TFIIE was diluted to 0.3 mg/ml in 20 mM Tris–HCl (pH 7.4) and 150 mM NaCl and processed as described (Adrian *et al*, 1998). Images were recorded under low-dose conditions at 43,900 magnification and at defocus values ranging from 0.5 to 1.2 μm, with an FEI Tecnai 20 TEM operating at 200 kV.

The micrographs were digitized at a pixel spacing of 0.3 nm using a drum scanner (Primescan D7100, Heidelberg, Germany). Image analysis was performed using the IMAGIC software package (van Heel *et al*, 1996) as described earlier (De Carlo *et al*, 2003). The images of cryo-negatively stained TFIIE were contrast transfer function corrected by phase inversion. All data sets were analysed independently and no common references were used for alignment or angular assignment. The resolution was estimated from the Fourier shell correlation function obtained by comparing two independent reconstructions, generated by splitting randomly the data set in half, according to the 0.145 cutoff criterion (Rosenthal & Henderson, 2003).

Supplementary information is available at *EMBO reports* online (http://www.emboreports.org).

ACKNOWLEDGEMENTS

We are grateful to C. Birck for help with ultracentrifugation. This work was supported by the Institut National de la Santé et de la Recherche Médicale, the Centre National pour la Recherche Scientifique, the Association pour la Recherche sur le Cancer (ARC), The European SPINE program, QLG2-CT-00988 and the European Union Grant RTN2-2001-00026. M.U. and A.J. were supported by ARC fellowships.

REFERENCES

Adrian M, Dubochet J, Fuller SD, Harris JR (1998) Cryo-negative staining. *Micron* **29:** 145–160

Bushnell DA, Bamdad C, Kornberg RD (1996) A minimal set of RNA polymerase II transcription protein interactions. *J Biol Chem* **271:** 20170–20174

De Carlo S, El Bez C, Alvarez-Rua C, Borge J, Dubochet J (2002) Cryo-negative staining reduces electron-beam sensitivity of vitrified biological particles. *J Struct Biol* **138:** 216–226

De Carlo S, Carles C, Riva M, Schultz P (2003) Cryo-negative staining reveals conformational flexibility within yeast RNA polymerase I. *J Mol Biol* **329:** 891–902

Forget D, Langelier MF, Therien C, Trinh V, Coulombe B (2004) Photo-cross-linking of a purified preinitiation complex reveals central roles for the RNA polymerase II mobile clamp and TFIIE in initiation mechanisms. *Mol Cell Biol* **24:** 1122–1131

Fribourg S, Romier C, Werten S, Gangloff YG, Poterszman A, Moras D (2001) Dissecting the interaction network of multiprotein complexes by pairwise coexpression of subunits in *E. coli*. *J Mol Biol* **306:** 363–373

Hayashi K, Watanabe T, Tanaka A, Furumoto T, Sato-Tsuchiya C, Kimura M, Yokoi M, Ishihama A, Hanaoka F, Ohkuma Y (2005) Studies of *Schizosaccharomyces pombe* TFIIE indicate conformational and functional changes in RNA polymerase II at transcription initiation. *Genes Cells* **10:** 207–224

Itoh Y, Unzai S, Sato M, Nagadoi A, Okuda M, Nishimura Y, Akashi S (2005) Investigation of molecular size of transcription factor TFIIE in solution. *Proteins* **279:** 51395–51403

Kim TK, Ebright RH, Reinberg D (2000) Mechanism of ATP-dependent promoter melting by transcription factor IIH. *Science* **288:** 1418–1422

Leuther KK, Bushnell DA, Kornberg RD (1996) Two-dimensional crystallography of T. *Cell* **85:** 773–779

Lu H, Zawel L, Fisher L, Egly JM, Reinberg D (1992) Human general transcription factor IIH phosphorylates the C-terminal domain of RNA polymerase II. *Nature* **358:** 641–645

Meinhart A, Blobel J, Cramer P (2003) An extended winged helix domain in general transcription factor E/IIEα. *J Biol Chem* **278:** 48267–48274

Ohkuma Y, Roeder RG (1994) Regulation of TFIIH ATPase and kinase activities by TFIIE during active initiation complex formation. *Nature* **368:** 160–163

Ohkuma Y, Sumimoto H, Horikoshi M, Roeder RG (1990) Factors involved in specific transcription by mammalian RNA polymerase II: purification and characterization of general transcription factor TFIIE. *Proc Natl Acad Sci USA* **87:** 9163–9167

Ohkuma Y, Hashimoto S, Wang CK, Horikoshi M, Roeder RG (1995) Analysis of the role of TFIIE in basal transcription and TFIIH-mediated carboxy-terminal domain phosphorylation through structure–function studies of TFIIE-α. *Mol Cell Biol* **15:** 4856–4866

Okamoto T, Yamamoto S, Watanabe Y, Ohta T, Hanaoka F, Roeder RG, Ohkuma Y (1998) Analysis of the role of TFIIE in transcriptional regulation through structure–function studies of the TFIIEβ subunit. *J Biol Chem* **273:** 19866–19876

Okuda M, Tanaka A, Arai Y, Satoh M, Okamura H, Nagadoi A, Hanaoka F, Ohkuma Y, Nishimura Y (2004) A novel zinc finger structure in the large subunit of human general transcription factor TFIIE. *J Biol Chem* **279:** 51395–51403

Okuda M, Watanabe Y, Okamura H, Hanaoka F, Ohkuma Y, Nishimura Y (2000) Structure of the central core domain of TFIIEβ with a novel double-stranded DNA-binding surface. *EMBO J* **19:** 1346–1356

Orphanides G, Lagrange T, Reinberg D (1996) The general transcription factors of RNA polymerase II. *Genes Dev* **10:** 2657–2683

Robert F, Forget D, Li J, Greenblatt J, Coulombe B (1996) Localization of subunits of transcription factors IIE and IIF immediately upstream of the transcriptional initiation site of the adenovirus major late promoter. *J Biol Chem* **271:** 8517–8520

Roeder RG (1996) The role of general initiation factors in transcription by RNA polymerase II. *Trends Biochem Sci* **21:** 327–335

Rosenthal PB, Henderson R (2003) Optimal determination of particle orientation, absolute hand, and contrast loss in single-particle electron cryomicroscopy. *J Mol Biol* **333:** 721–745

Sayre MH, Tschochner H, Kornberg RD (1992) Purification and properties of *Saccharomyces cerevisiae* RNA polymerase II general initiation factor a. *J Biol Chem* **267:** 23383–23387

van Heel M, Harauz G, Orlova EV (1996) A new generation of the IMAGIC image processing system. *J Struct Biol* **116:** 17–24

Van Mullem V, Wery M, Werner M, Vandenhaute J, Thuriaux P (2002) The Rpb9 subunit of RNA polymerase II binds transcription factor TFIIE and interferes with the SAGA and elongator histone acetyltransferases. *J Biol Chem* **277:** 10220–10225

Wichertjes T, Keegstra W, Neuteboom B, Hazes B, Beintema JJ, Van Bruggen EF (1989) Crystallization properties and structure of *Panulirus interruptus* haemocyanin. *Eur J Biochem* **184:** 287–296